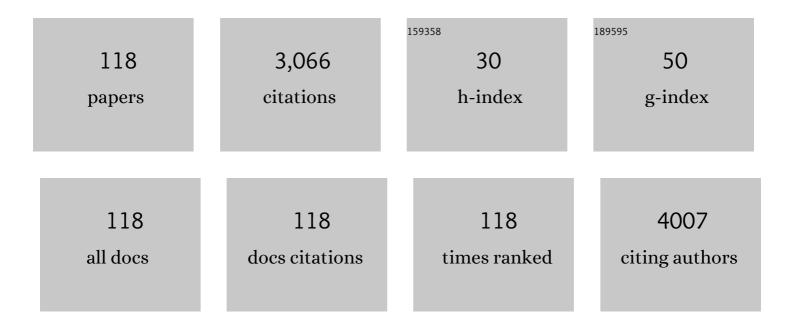
Yongfeng Li

List of Publications by Year in descending order

Source: https://exaly.com/author-pdf/7048989/publications.pdf Version: 2024-02-01



YONGFENC LL

#	Article	IF	CITATIONS
1	Influence mechanism of Cu+/(Cu++Cu2+) ratio in Cu-Zn-Sn-S precursor solution on performance of Cu2ZnSn(S,Se)4 solar cells. Solar Energy, 2022, 231, 775-783.	2.9	5
2	Role of zinc tin oxide passivation layer at back electrode interface in improving efficiency of Cu2ZnSn(S,Se)4 solar cells. Superlattices and Microstructures, 2022, 163, 107133.	1.4	4
3	Efficiency enhancement of Cu2ZnSn(S, Se)4 solar cells by addition a CuSe intermediate layer between Cu2ZnSn(S, Se)4 and Mo electrode. Journal of Alloys and Compounds, 2022, 911, 165056.	2.8	11
4	A self-powered high performance UV-Vis-NIR broadband photodetector based on β-Bi ₂ O ₃ nanoparticles through defect engineering. Journal of Materials Chemistry C, 2022, 10, 8364-8372.	2.7	16
5	Improvement of Photovoltaic Performance of Cu ₂ ZnSn(S,Se) ₄ Solar Cells by Modification of Back Electrode Interface with Amorphous Boron Nitride. Advanced Materials Interfaces, 2022, 9, .	1.9	4
6	Single Exposure to Cocaine Impairs Reinforcement Learning by Potentiating the Activity of Neurons in the Direct Striatal Pathway in Mice. Neuroscience Bulletin, 2021, 37, 1119-1134.	1.5	6
7	N–SrTiO3/p-GaN heterojunctions: A white light-emitting diode with a broad luminescence spectrum. Materials Science in Semiconductor Processing, 2021, 126, 105659.	1.9	7
8	Preparation and characterization of Ag2ZnSn(S,Se)4 and its application in improvement of power conversion efficiency of Cu2ZnSn(S,Se)4-based solar cells. Ceramics International, 2021, 47, 34473-34480.	2.3	4
9	Mechanism of enhanced power conversion efficiency of Cu2ZnSn(S, Se)4 solar cell by cadmium surface diffusion doping. Journal of Alloys and Compounds, 2021, 876, 160160.	2.8	22
10	Tuning optical and electrical properties of TixSn1â^'xO2 alloy thin films with dipole-forbidden transition via band gap and defect engineering. Journal of Alloys and Compounds, 2021, 885, 160974.	2.8	5
11	Doping Behavior of Zn in CdS and Its Effect on the Power Conversion Efficiency of the Cu ₂ ZnSn(S, Se) ₄ Solar Cell. Journal of Physical Chemistry C, 2021, 125, 27449-27457.	1.5	7
12	Modulation of Field-Effect Passivation at the Back Electrode Interface Enabling Efficient Kesterite-Type Cu ₂ ZnSn(S,Se) ₄ Thin-Film Solar Cells. ACS Applied Materials & Interfaces, 2020, 12, 38163-38174.	4.0	18
13	Influence of WSe2 buffer layer at back electrode on performance of Cu2ZnSn(S,Se)4 solar cells. Solar Energy, 2020, 199, 128-135.	2.9	18
14	Cation impurity-defect complex induced ferromagnetism and hopping conduction in Sb-doped ZnO synthesized under high pressure. Journal of Alloys and Compounds, 2020, 823, 153713.	2.8	4
15	Self-Organized Back Surface Field to Improve the Performance of Cu ₂ ZnSn(S,Se) ₄ Solar Cells by Applying P-Type MoSe ₂ :Nb to the Back Electrode Interface. ACS Applied Materials & Interfaces, 2019, 11, 31851-31859.	4.0	24
16	Electron doping of Sr ₂ FeMoO _{6â^'δ} as high performance anode materials for solid oxide fuel cells. Journal of Materials Chemistry A, 2019, 7, 733-743.	5.2	42
17	Structural, electrical, and optical properties of Ag2ZnSnSe4 for photodetection application. Journal of Applied Physics, 2019, 125, .	1.1	15
18	Synthesis and characterizations of Cu2MgSnS4 thin films with different sulfuration temperatures. Materials Letters, 2019, 242, 58-61.	1.3	22

#	Article	IF	CITATIONS
19	Synthesis and characterization of WB2-WB3-B4C hard composites. International Journal of Refractory Metals and Hard Materials, 2019, 82, 268-272.	1.7	15
20	Influencing mechanism of cationic ratios on efficiency of Cu2ZnSn(S,Se)4 solar cells fabricated with DMF-based solution approach. Solar Energy Materials and Solar Cells, 2019, 195, 55-62.	3.0	20
21	Improving the Back Electrode Interface Quality of Cu ₂ ZnSn(S,Se) ₄ Thin-Film Solar Cells Using a Novel CuAlO ₂ Buffer Layer. ACS Applied Energy Materials, 2019, 2, 2230-2237.	2.5	31
22	Ultraviolet electroluminescence from nanostructural SnO2-based heterojunction with high-pressure synthesized Li-doped ZnO as a hole source. Ceramics International, 2019, 45, 4392-4397.	2.3	7
23	Improvement of the photovoltaic performance of Ag-alloyed Cu2ZnSn(S,Se)4-based solar cells by optimizing the selenization temperature. Superlattices and Microstructures, 2019, 125, 287-294.	1.4	5
24	Surface sulfurization of ZnO/ZnS core shell nanowires and shell layers dependent optical properties. Journal of Materials Science: Materials in Electronics, 2018, 29, 7924-7929.	1.1	3
25	Surface State Passivation and Optical Properties Investigation of GaSb via Nitrogen Plasma Treatment. ACS Omega, 2018, 3, 4412-4417.	1.6	15
26	Localized-State-Dependent Electroluminescence from ZnO/ZnS Core–Shell Nanowires–GaN Heterojunction. ACS Applied Nano Materials, 2018, 1, 1641-1647.	2.4	13
27	Improvement of the photovoltaic performance of Cu ₂ ZnSn(S _{<i>x</i>) Tj ETQq1 1 0.78431 solution. Journal Physics D: Applied Physics, 2018, 51, 105103.}	4 rgBT /Ον 1.3	erlock 10 Tf 5 10
28	Structure, optical and electrical properties of (Cu1-xAgx)2ZnSn(S,Se)4 alloy thin films for photovoltaic application. Materials Science in Semiconductor Processing, 2018, 81, 54-59.	1.9	17
29	Photoresponse enhancement in SnO2-based ultraviolet photodetectors via coupling with surface plasmons of Ag particles. Journal of Alloys and Compounds, 2018, 748, 398-403.	2.8	27
30	Modification of back electrode with WO3 layer and its effect on Cu2ZnSn(S,Se)4-based solar cells. Superlattices and Microstructures, 2018, 113, 328-336.	1.4	7
31	Enhanced efficiency of Cu ₂ ZnSn(S,Se) ₄ solar cells <i>via</i> anti-reflectance properties and surface passivation by atomic layer deposited aluminum oxide. RSC Advances, 2018, 8, 19213-19219.	1.7	6
32	First-principles investigations on extrinsic acceptor defects in alkaline-earth metal and N doped CuAlO2. Physica B: Condensed Matter, 2018, 547, 38-47.	1.3	2
33	Behavior of indium alloying with Cu2ZnSn(S,Se)4 and its effect on performances of Cu2ZnSn(S,Se)4-based solar cell. Journal of Alloys and Compounds, 2018, 767, 439-447.	2.8	13
34	Effects of etching on surface structure of Cu2ZnSn(S,Se)4 absorber and performance of solar cell. Solar Energy, 2018, 173, 696-701.	2.9	11
35	Investigation of localized and delocalized excitons in ZnO/ZnS core-shell heterostructured nanowires. Nanophotonics, 2017, 6, 1093-1100.	2.9	14
36	Role of nitrogen-related complex in stabilizing ferromagnetic ordering in a rare-earth and nitrogen codoped ZnO. Ceramics International, 2017, 43, 6013-6018.	2.3	8

#	Article	IF	CITATIONS
37	A versatile strategy for fabricating various Cu ₂ ZnSnS ₄ precursor solutions. Journal of Materials Chemistry C, 2017, 5, 3035-3041.	2.7	20
38	Band offsets of Ag2ZnSnSe4/CdS heterojunction: An experimental and first-principles study. Journal of Applied Physics, 2017, 121, .	1.1	22
39	Effect of Cd content and sulfurization on structures and properties of Cd doped Cu2SnS3 thin films. Journal of Alloys and Compounds, 2017, 721, 92-99.	2.8	14
40	Significantly enhancing back contact adhesion and improving stability of Cu2(Zn,Cd)Sn(S,Se)4 solar cell by a rational carbon doping strategy. Journal of Alloys and Compounds, 2017, 710, 403-408.	2.8	16
41	Shallow Acceptor State in Mg-Doped CuAlO ₂ and Its Effect on Electrical and Optical Properties: An Experimental and First-Principles Study. ACS Applied Materials & Interfaces, 2017, 9, 12608-12616.	4.0	35
42	Giant enhancement of ultraviolet near-band-edge emission from a wide-bandgap oxide with dipole-forbidden bandgap transition. Journal of Alloys and Compounds, 2017, 705, 492-496.	2.8	5
43	Fabrication of Cu ₂ MSnS ₄ (M = Co ²⁺ , Ni ²⁺) nanocrystal thin films and their application in photodetectors. New Journal of Chemistry, 2017, 41, 685-691.	1.4	23
44	Visible-blind ultraviolet photodetector based on p-Cu2CdSnS4/n-ZnS heterojunction with a type-I band alignment. Journal of Applied Physics, 2016, 120, .	1.1	11
45	Impact of sequential annealing step on the performance of Cu2ZnSn(S,Se)4 thin film solar cells. Superlattices and Microstructures, 2016, 95, 149-158.	1.4	6
46	Band alignment at a MgO/GaSb heterointerface using x-ray photoelectron spectroscopy measurements. Materials Research Express, 2016, 3, 076402.	0.8	2
47	Synthesis of Antimony Nanotubes via Facile Template-Free Solvothermal Reactions. Nanoscale Research Letters, 2016, 11, 486.	3.1	8
48	Determination of band offset in MgO/InP heterostructure by X-ray photoelectron spectroscopy. Vacuum, 2016, 134, 136-140.	1.6	9
49	Highly spectrum-selective near-band-edge ultraviolet photodiode based on indium oxide with dipole-forbidden bandgap transition. Ceramics International, 2016, 42, 8017-8021.	2.3	5
50	Ultraviolet Electroluminescence from ZnS@ZnO Core–Shell Nanowires/p-GaN Introduced by Exciton Localization. ACS Applied Materials & Interfaces, 2016, 8, 1661-1666.	4.0	42
51	Effect of Mg doping on optical and electrical properties of SnO2 thin films: An experiment and first-principles study. Ceramics International, 2016, 42, 5299-5303.	2.3	26
52	Effect of doping behaviors of Ag and S on the formation of p-type Ag–S co-doped ZnO film by a modified hydrothermal method. Thin Solid Films, 2016, 600, 13-18.	0.8	7
53	Synthesis and characterization of noble metal borides: RuB (x> 1). Materials Research Bulletin, 2016, 74, 188-191.	2.7	12
54	Nanomaterials for Energy-Efficient Applications. Journal of Nanomaterials, 2015, 2015, 1-2.	1.5	3

#	Article	IF	CITATIONS
55	Photoluminescence Properties of the GaSb Nanostructures Irradiated by Femtosecond Laser. Nanoscience and Nanotechnology Letters, 2015, 7, 117-120.	0.4	1
56	Mechanism of effect of intrinsic defects on electrical and optical properties of Cu ₂ CdSnS ₄ : an experimental and first-principles study. Journal Physics D: Applied Physics, 2015, 48, 445105.	1.3	16
57	Band alignments at interface of Cu2ZnSnS4/ZnO heterojunction: An X-ray photoelectron spectroscopy and first-principles study. Journal of Alloys and Compounds, 2015, 628, 293-297.	2.8	26
58	Recovering near-band-edge ultraviolet responses in a wide-bandgap oxide with dipole-forbidden bandgap transition. Journal of Alloys and Compounds, 2015, 649, 625-629.	2.8	6
59	Alternative Spectral Photoresponse in a <i>p</i> -Cu ₂ ZnSnS ₄ / <i>n</i> -GaN Heterojunction Photodiode by Modulating Applied Voltage. ACS Applied Materials & Interfaces, 2015, 7, 16653-16658.	4.0	22
60	Device Performance of the Mott Insulator <mml:math xmlns:mml="http://www.w3.org/1998/Math/MathML" display="inline"><mml:mrow><mml:msub><mml:mrow><mml:mi>LaVO</mml:mi></mml:mrow><mml:mrow><r a Photovoltaic Material. Physical Review Applied, 2015, 3, .</r </mml:mrow></mml:msub></mml:mrow></mml:math 	nml:mn>3	</td
61	Fabrication, characterization and application of Cu2ZnSn(S,Se)4 absorber layer via a hybrid ink containing ball milled powders. Journal of Alloys and Compounds, 2015, 643, 152-158.	2.8	16
62	Experimental and first-principles study of photoluminescent and optical properties of Na-doped CuAlO ₂ : the role of the Na _{Al} -2Na _{<i>i</i>} complex. Journal Physics D: Applied Physics, 2015, 48, 335102.	1.3	9
63	A facile route to realize ultraviolet emission in a nano-engineered SnO ₂ -based light-emitting diode. Journal Physics D: Applied Physics, 2015, 48, 465103.	1.3	13
64	Effect of Al Diffusion on Electrical and Photoluminescent Properties of Mg _x Zn _{1–<i>x</i>} O Alloy Films Fabricated on Sapphire Substrates. Nanoscience and Nanotechnology Letters, 2015, 7, 111-116.	0.4	1
65	Surface Periodic Nanostructure of <i>p</i> -GaSb Irradiated by Femtosecond Laser and Optical Properties Research. Nanoscience and Nanotechnology Letters, 2015, 7, 1-5.	0.4	9
66	An experimental and first-principles study on band alignments at interfaces of Cu ₂ ZnSnS ₄ /CdS/ZnO heterojunctions. Journal Physics D: Applied Physics, 2014, 47, 075304.	1.3	44
67	Influence of Ag–S codoping on silver chemical states and stable p-type conduction behavior of the ZnO films. Ceramics International, 2014, 40, 2161-2167.	2.3	11
68	Electrostatic Modulation of LaAlO ₃ /SrTiO ₃ Interface Transport in an Electric Double‣ayer Transistor. Advanced Materials Interfaces, 2014, 1, 1300001.	1.9	75
69	Structural, electronic and optical properties of Cd x Zn 1â^'x S alloys from first-principles calculations. Physics Letters, Section A: General, Atomic and Solid State Physics, 2014, 378, 3382-3388.	0.9	6
70	Wavelength-Tuned Light Emission via Modifying the Band Edge Symmetry: Doped SnO ₂ as an Example. Journal of Physical Chemistry C, 2014, 118, 6365-6371.	1.5	28
71	Er60Ni132: A new structure from the Ni occupied the 4b sites in cubic laves superstructure synthesized under high pressure and high temperature. Intermetallics, 2014, 55, 195-198.	1.8	0
72	Surface state and optical property of sulfur passivated InP. Materials Science in Semiconductor Processing, 2014, 17, 33-37.	1.9	22

....

#	ARTICLE	IF	CITATIONS
73	Chemical states of gold doped in ZnO films and its effect on electrical and optical properties. Journal of Alloys and Compounds, 2014, 585, 479-484.	2.8	26
74	Shallow Donor Ionization Energy in Sn-Doped ZnO Nanobelts. Nanoscience and Nanotechnology Letters, 2014, 6, 887-891.	0.4	2
75	Photoinduced phase transition and relaxation in bare SrTiO3 single crystals. Journal of Applied Physics, 2013, 114, .	1.1	16
76	Electronic and optical properties of kesterite Cu2ZnSnS4 under in-plane biaxial strains: First-principles calculations. Physics Letters, Section A: General, Atomic and Solid State Physics, 2013, 377, 2398-2402.	0.9	25
77	Chemical State, Site, Solid Solubility, and Magnetism of Fe in the Ferropericlase (Mg1–x Fe x)O Produced by Ball Milling of MgO and Fe. Metallurgical and Materials Transactions A: Physical Metallurgy and Materials Science, 2013, 44, 4551-4557.	1.1	2
78	A comparative study on electroluminescence from ZnO-based double heterojunction light emitting diodes grown on different lattice mismatch substrates. Journal of Alloys and Compounds, 2013, 575, 233-238.	2.8	27
79	High pressure synthesis and characterization of noble metal nitride IrNx. Materials Letters, 2013, 107, 382-385.	1.3	5
80	Bandgap engineering of Cu2CdxZn1â^'xSnS4 alloy for photovoltaic applications: A complementary experimental and first-principles study. Journal of Applied Physics, 2013, 114, .	1.1	88
81	Conversion mechanism of conductivity of phosphorus-doped ZnO films induced by post-annealing. Journal of Applied Physics, 2013, 113, 193105.	1.1	11
82	Effects of S on solid solubility of Ag and electrical properties of Ag-doped ZnO films grown by radio frequency magnetron sputtering. Journal of Alloys and Compounds, 2013, 550, 479-482.	2.8	14
83	Ultraviolet electroluminescence from n-ZnO/p-NiO heterojunction light-emitting diode. Journal of Luminescence, 2013, 134, 240-243.	1.5	48
84	Electrostatic tuning of Kondo effect in a rare-earth-doped wide-band-gap oxide. Physical Review B, 2013, 87, .	1.1	49
85	Experimental and first-principles study of ferromagnetism in Mn-doped zinc stannate nanowires. Journal of Applied Physics, 2013, 114, .	1.1	7
86	Effects of magnesium on phosphorus chemical states and <i>p</i> -type conduction behavior of phosphorus-doped ZnO films. Journal of Chemical Physics, 2013, 138, 034704.	1.2	7
87	Tunable photovoltaic effect and solar cell performance of self-doped perovskite SrTiO3. AIP Advances, 2012, 2, .	0.6	28
88	Role of donor-acceptor complexes and impurity band in stabilizing ferromagnetic order in Cu-doped SnO2 thin films. Applied Physics Letters, 2012, 100, 172402.	1.5	71
89	Phase Selection Enabled Formation of Abrupt Axial Heterojunctions in Branched Oxide Nanowires. Nano Letters, 2012, 12, 275-280.	4.5	27
90	The effect of annealing temperature on electrical properties of Au/n-GaSb Schottky contacts. , 2012, , .		0

#	Article	IF	CITATIONS
91	Hole-mediated ferromagnetic enhancement and stability in Cu-doped ZnOS alloy thin films. Journal Physics D: Applied Physics, 2012, 45, 075002.	1.3	7
92	Realizing a SnO2-based ultraviolet light-emitting diode via breaking the dipole-forbidden rule. NPG Asia Materials, 2012, 4, e30-e30.	3.8	137
93	Deterministic conversion between memory and threshold resistive switching via tuning the strong electron correlation. Scientific Reports, 2012, 2, 442.	1.6	110
94	Evidence of cation vacancy induced room temperature ferromagnetism in Li-N codoped ZnO thin films. Applied Physics Letters, 2011, 99, 182503.	1.5	47
95	Defect-induced magnetism in undoped wide band gap oxides: Zinc vacancies in ZnO as an example. AIP Advances, 2011, 1, .	0.6	179
96	Interface-dependent rectifying TbMnO3-based heterojunctions. AIP Advances, 2011, 1, .	0.6	22
97	Tuning magnetoresistance and exchange coupling in ZnO by doping transition metals. Applied Physics Letters, 2011, 99, 222503.	1.5	48
98	Bound magnetic polarons and p-d exchange interaction in ferromagnetic insulating Cu-doped ZnO. Applied Physics Letters, 2011, 98, .	1.5	116
99	Doping efficiency, optical and electrical properties of nitrogen-doped ZnO films. Journal of Applied Physics, 2011, 109, .	1.1	39
100	Tuning ferromagnetism in MgxZn1â^'xO thin films by band gap and defect engineering. Applied Physics Letters, 2010, 97, .	1.5	90
101	Influence of oxygen/argon ratio on structural, electrical and optical properties of Ag-doped ZnO thin films. Journal of Crystal Growth, 2010, 312, 1813-1816.	0.7	23
102	Oxygen partial pressure dependence of the properties of MgZnO thin films during annealing. Journal of Materials Science, 2010, 45, 6206-6211.	1.7	4
103	MgZnO/ZnO p–n junction UV photodetector fabricated on sapphire substrate by plasma-assisted molecular beam epitaxy. Solid State Sciences, 2010, 12, 1567-1569.	1.5	42
104	Structure, luminescence and electrical properties of ZnO thin films annealed in H2 and H2O ambient: A comparative study. Thin Solid Films, 2010, 518, 3923-3928.	0.8	13
105	Investigation on the formation mechanism of p-type Li–N dual-doped ZnO. Applied Physics Letters, 2010, 97, 222101.	1.5	57
106	Influence of Zn/O ratio on structural, electrical and optical properties of ZnO thin films fabricated by plasma-assisted molecular beam epitaxy. Journal of Alloys and Compounds, 2010, 503, 155-158.	2.8	26
107	p-Type MgZnO thin films grown using N delta-doping by plasma-assisted molecular beam epitaxy. Journal of Alloys and Compounds, 2010, 504, 484-487.	2.8	19
108	A Template and Catalyst-Free Metal-Etching-Oxidation Method to Synthesize Aligned Oxide Nanowire Arrays: NiO as an Example. ACS Nano, 2010, 4, 4785-4791.	7.3	44

#	Article	IF	CITATIONS
109	X-ray photoelectron spectroscopy measurement of n-ZnO/p-NiO heterostructure valence-band offset. Applied Physics Letters, 2009, 94, .	1.5	84
110	Annealing temperature dependent electrical and optical properties of ZnO and MgZnO films in hydrogen ambient. Applied Surface Science, 2009, 255, 6745-6749.	3.1	34
111	Surface morphology, structural and optical properties of polar and non-polar ZnO thin films: A comparative study. Journal of Crystal Growth, 2009, 311, 4398-4401.	0.7	24
112	Ultraviolet photodiode based on p-Mg _{0.2} Zn _{0.8} O/n-ZnO heterojunction with wide response range. Journal Physics D: Applied Physics, 2009, 42, 105102.	1.3	31
113	Influence of hydrostatic pressure on the native point defects in wurtzite ZnO: Ab initio calculation. Physics Letters, Section A: General, Atomic and Solid State Physics, 2008, 372, 5077-5082.	0.9	11
114	Valence-band offset of epitaxial ZnOâ^•MgO (111) heterojunction determined by x-ray photoelectron spectroscopy. Applied Physics Letters, 2008, 92, .	1.5	59
115	Biaxial stress-dependent optical band gap, crystalline, and electronic structure in wurtzite ZnO: Experimental and <i>ab initio</i> study. Journal of Applied Physics, 2008, 104, .	1.1	57
116	Effect on nitrogen acceptor as Mg is alloyed into ZnO. Applied Physics Letters, 2008, 92, 062110.	1.5	34
117	Characterization of biaxial stress and its effect on optical properties of ZnO thin films. Applied Physics Letters, 2007, 91, 021915.	1.5	96
118	Realization of p-type conduction in undoped MgxZn1â^'xO thin films by controlling Mg content. Applied Physics Letters, 2007, 91, 232115.	1.5	58